

Astrometric orbits of S_{B9} stars

S. Jancart, A. Jorissen*, C. Babusiaux, and D. Pourbaix**

Institut d'Astronomie et d'Astrophysique, Université Libre de Bruxelles, C.P. 226, Boulevard du Triomphe, B-1050 Bruxelles, Belgium

Received date; accepted date

Abstract. Hipparcos Intermediate Astrometric Data (IAD) have been used to derive astrometric orbital elements for spectroscopic binaries from the newly released *Ninth Catalogue of Spectroscopic Binary Orbits* (S_{B9}). This endeavour is justified by the fact that (i) the astrometric orbital motion is often difficult to detect without the prior knowledge of the spectroscopic orbital elements, and (ii) such knowledge was not available at the time of the construction of the Hipparcos Catalogue for the spectroscopic binaries which were recently added to the S_{B9} catalogue.

Among the 1374 binaries from S_{B9} which have an HIP entry (excluding binaries with visual companions, or DMSA/C in the Double and Multiple Stars Annex), 282 have detectable orbital astrometric motion (at the 5% significance level). Among those, only 70 have astrometric orbital elements that are reliably determined (according to specific statistical tests), and for the first time for 20 systems. This represents a 8.5% increase of the number of astrometric systems with known orbital elements (The Double and Multiple Systems Annex contains 235 of those DMSA/O systems).

The detection of the astrometric orbital motion when the Hipparcos IAD are supplemented by the spectroscopic orbital elements is close to 100% for binaries with only one visible component, provided that the period is in the 50 - 1000 d range and the parallax is > 5 mas. This result is an interesting testbed to guide the choice of algorithms and statistical tests to be used in the search for astrometric binaries during the forthcoming ESA Gaia mission.

Finally, orbital inclinations provided by the present analysis have been used to derive several astrophysical quantities. For instance, 29 among the 70 systems with reliable astrometric orbital elements involve main sequence stars for which the companion mass could be derived. Some interesting conclusions may be drawn from this new set of stellar masses, like the enigmatic nature of the companion to the Hyades F dwarf HIP 20935. This system has a mass ratio of 0.98 but the companion remains elusive.

Key words. Astrometry – Binaries: spectroscopic – Binaries: astrometric – Stars: mass

1. Introduction

The *Ninth Catalogue of Spectroscopic Binary Orbits* (S_{B9} ; Pourbaix et al. 2004, available at <http://sb9.astro.ulb.ac.be>) continues the series of compilations of spectroscopic orbits carried out over the past 35 years by Batten and collaborators. As of 2004 May 1st, the new Catalogue holds orbits for 2386 systems. The *Hipparcos Intermediate Astrometric Data* (IAD; van Leeuwen & Evans 1998) offer good prospects to derive astrometric orbits for those binaries. Astrometric orbits are often difficult to extract from the IAD without prior knowledge of at least some among the orbital elements (e.g., Pourbaix 2004). As an illustration of the difficulty, only 45 out of 235 Double and Multiple Systems Annex Orbital solutions [DMSA/O, see ESA (1997) and Lindegren et al. (1997)] were derived from scratch. For those S_{B9} binaries whose orbit has become available after the publication of the Hipparcos Catalogue, new astrometric orbital elements may be expected from the re-processing of their IAD. This is the major aim of the present paper, which

belongs to a series devoted to the re-processing of the IAD for binaries (Pourbaix & Jorissen 2000; Pourbaix & Boffin 2003).

One of the major challenges facing astronomers studying binaries and extrasolar planets is to get the inclination of the companion orbit in order to derive the component masses. The orbital inclinations will be provided in this paper for 70 systems (Sect. 5). To get the component masses requires moreover the system to be spectroscopic binary with 2 observable spectra (SB2). Unfortunately, SB2 systems are not favourable targets to detect their astrometric orbital motion using the IAD. When the component's brightnesses do not differ much (less than about 1 magnitude), the orbital motion of the photocenter of the system around its barycenter might not be large enough to allow detection (see Eq. 8 below). This means that the astrometric orbit cannot in general be derived from the IAD for SB2 systems (neither can the component solutions – DMSA/C – when available, be reprocessed using the IAD, because the abscissa residuals of DMSA/C entries turn out to be abnormally large, even for non-binary stars), thus compromising our ability to derive stellar masses in a fully self-consistent way in the present paper. This difficulty will be circumvented by the use of the mass – luminosity relationship for main sequence stars, thus

* Senior Research Associate, F.N.R.S., Belgium

** Research Associate, F.N.R.S., Belgium

allowing us to derive at least the *companion's* mass (Sect. 6.1). This information will then be combined with the position of the system in the eccentricity – period diagram to diagnose post-mass-transfer systems (Sect. 6.2).

Another important motivation of the present paper is to test on the IAD, algorithms designed (i) to detect astrometric binaries and (ii) to determine their orbital parameters in the framework of the future ESA cornerstone mission Gaia. IAD are indeed very similar to what will be available at some stage of the Gaia data reduction process. The fit of an orbital model to the IAD is greatly helped with a partial knowledge of the orbital elements, coming from the spectroscopic orbit (Pourbaix 2004). In the present context, orbital elements like eccentricity e , orbital period P and one epoch of periastron passage T_0 are provided by the spectroscopic orbits listed in S_{B^9} . With Gaia, these elements may come (in the most favourable circumstances) from the spectroscopic orbit derived from the on-board radial-velocity measurements.

2. The Hipparcos data

During 3 years and for about 118 000 stars, the Hipparcos satellite (ESA 1997) measured tens of abscissae per star, *i.e.*, 1-dimensional positions along precessing great circles. Corrections like chromaticity effects, satellite attitude, ... were then applied to these abscissae. It was decided that the residuals (Δv) of these corrected abscissae (with respect to a 5-parameter single-star astrometric model) would be released together with the Hipparcos Catalogue. They constitute the IAD (van Leeuwen & Evans 1998). In order to make the interpretation of these residuals unambiguous, the released values were all derived with the single-star model, no matter what model was used for that catalogue entry. It is then possible for anybody to fit any model to these IAD to seek further reduction of the residuals.

2.1. The orbital model

The fit of the IAD with an orbital model is achieved through a χ^2 minimization:

$$\chi^2 = (\Delta v - \sum_k \frac{\partial v}{\partial p_k} \Delta p_k - \sum_i \frac{\partial v}{\partial o_i} o_i)^t \mathbf{V}^{-1} (\Delta v - \sum_k \frac{\partial v}{\partial p_k} \Delta p_k - \sum_i \frac{\partial v}{\partial o_i} o_i), \quad (1)$$

where Δp_k is the correction applied to the original (astrometric) parameter p_k [where $(p_1, p_2, p_3, p_4, p_5) \equiv (\alpha, \delta, \varpi, \mu_{\alpha^*}, \mu_\delta)$], o_i are the orbital parameters and \mathbf{V} is the covariance matrix of the data. $\Delta v_j, \partial v_j / \partial p_k$, and \mathbf{V} ($j = 1, \dots, n; k = 1, \dots, 5$) and the Main Hipparcos solution are provided, n is the number of IAD available for the considered star [see van Leeuwen & Evans (1998) for details]. Equation

(1) thus reduces to

$$\chi^2 = (\Delta v - \sum_k \frac{\partial v}{\partial p_k} \Delta p_k - y \frac{\partial v}{\partial p_1} - x \frac{\partial v}{\partial p_2})^t \mathbf{V}^{-1} (\Delta v - \sum_k \frac{\partial v}{\partial p_k} \Delta p_k - y \frac{\partial v}{\partial p_1} - x \frac{\partial v}{\partial p_2}) \quad (2)$$

where (x, y) is the relative position of the photocenter with respect to the barycenter of the binary system given by

$$x = AX + FY$$

$$y = BX + GY$$

with

$$X = \cos E - e$$

$$Y = \sqrt{1 - e^2} \sin E.$$

A, B, F, G are the Thiele-Innes constants (describing the photocenter orbit), e is the eccentricity and E the eccentric anomaly.

2.2. Outliers screening

Even in the original processing, not all the observations were used to derive the astrometric solution. Some of the observations were flagged as outliers and simply ignored if their residuals exceeded three times the nominal (*a priori*) error for those measurements. These outlying observations are identified by lower case 'f' or 'n' flags in the IAD file (instead of upper case 'F' or 'N' flags, corresponding to processing by the FAST or NDAC consortium, respectively). Since the model (and therefore the residuals) is going to be revised, so must be the outliers. Because the Thiele-Innes model is a linear one (see Eq. 2), its solution is unique and it may therefore be used to screen out the outliers of the orbital model.

All observations are initially kept. The observation with the largest residual using the orbital model is removed and the model fitted again without it. If the original residual exceeds three times the standard deviation of the new residuals, the observation is definitively discarded (since the number of observations is always less than 300, random fluctuations should yield less than 1 observation with a residual larger than 3σ). The process is then repeated with the new largest residual, and so on. Otherwise, the observation is restored and the whole process is terminated.

A total of 3 486 observations (out of 84 766) are thus removed. 60% of these outliers turn out to come from the NDAC processing even though the two consortia essentially contribute for the same amount of data. The percentage of outliers is ten times larger than in the original Hipparcos processing.

3. The sample

Among the $\sim 118 000$ stars in the Hipparcos catalogue, some 17 918 were flagged as double and multiple systems (DMSA) and 235 of them, the so-called DMSA/O, have an orbital solution. Our sample consists of the S_{B^9} entries with an HIP number, excluding DMSA/C entries (*i.e.*, resolved binaries

not suited for IAD processing). The sample contains 1 374 $\text{HIP}+S_{B^9}$ entries which cover an extensive period and eccentricity range (see Figs. 1 and 2).

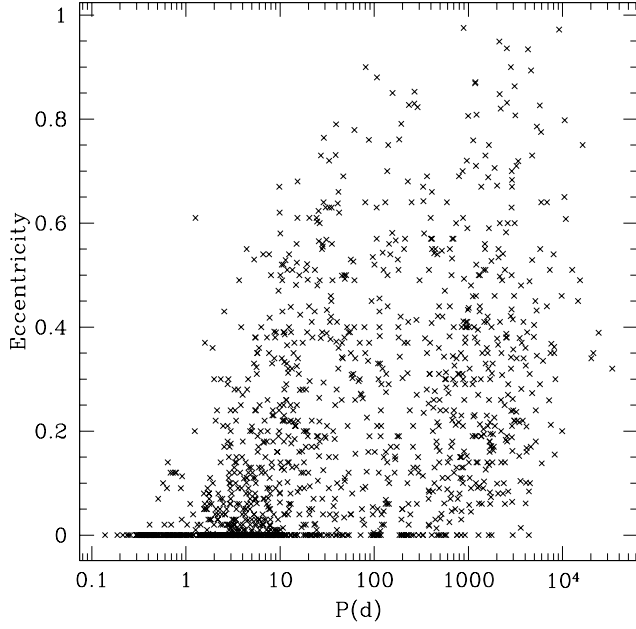


Fig. 1. Period-eccentricity diagram for the selected S_{B^9} objects with an HIP entry.

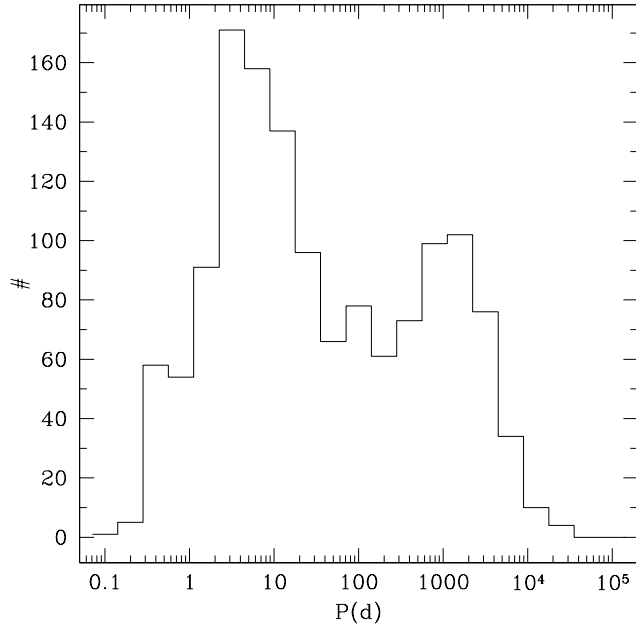


Fig. 2. Distribution of the orbital periods for the selected S_{B^9} objects with an HIP entry.

Even though a grade characterizes the quality of the spectroscopic orbits listed in S_{B^9} , those grades were not considered

a priori in the present processing, which uses the most recent orbit available. The quality of the spectroscopic orbit will be checked at the end of the process, in the discussion of Sect. 4 relative to the detection efficiency of the astrometric wobble.

4. Astrometric wobble detection

4.1. Detection assessment

We check whether an orbital motion lies hidden in the IAD using two mathematically equivalent methods of orbit determination, the Thiele-Innes and Campbell approaches. In both cases, the eccentricity, orbital period and the time of passage at periastron are taken from the spectroscopic orbit. For multiple systems, we always use the shortest period. This choice may not necessarily be the best one, but its validity is anyway assessed *a posteriori* by the ‘periodogram’ test (see below).

In the Thiele-Innes approach, the remaining four orbital parameters are derived through the Thiele-Innes constants A, B, F, G obtained from the χ^2 minimization of the linear model expressed by Eq. (2). The semi-major axis of the photocentric orbit (a_0), the inclination (i), the latitude of the ascending node (Ω) and the argument of the periastron (ω) (also known as *Campbell’s elements*) are then extracted from the Thiele-Innes constants, using standard formulae (Binnendijk 1960). In the Campbell approach, on the other hand, two more parameters, ω and the semi-amplitude of the primary’s radial-velocity curve K_1 are adopted from the spectroscopic orbit. Here, only two parameters of the photocentric orbit (i and Ω) are thus derived from the astrometry. This model is non-linear. The Campbell approach implicitly assumes that there is no light coming from the companion, since the spectroscopic elements constrain a_1 according to

$$a_1 \sin i = \varpi \frac{K_1 P \sqrt{1 - e^2}}{2\pi}. \quad (3)$$

The IAD, on the other hand, give access to the *photocentric* orbit characterized by a_0 , and we assume that $a_1 = a_0$. If this assumption does not hold, the solutions derived from the Thiele-Innes and Campbell approaches will be inconsistent, and will be rejected *a posteriori* by the consistency check described in Sect. 5.

We quantify the likelihood that there is an orbital wobble in the data with a F-test evaluating the significance of the decrease of the χ^2 resulting from the addition of four supplementary parameters (the four Thiele-Innes constants) in the orbital model (Pourbaix & Arenou 2001):

$$Pr_2 = Pr(F(4, n - 9) > \hat{F}), \quad (4)$$

where $\hat{F} = \frac{n-9}{4} \frac{\chi_S^2 - \chi_T^2}{\chi_T^2}$ follows a F -distribution with $(4, n - 9)$ degrees of freedom, n is the number of available IAD for the considered star, χ_T^2 and χ_S^2 are the χ^2 values associated with the orbital and single-star models, respectively. Pr_2 is the probability that the random variable $F(4, n - 9)$ exceeds the given value \hat{F} , it is thus the first-kind risk associated with the rejection of the null hypothesis ‘*there is no orbital wobble present in the data*’. The Pr_2 test is a χ^2 -ratio test; it is therefore insensitive to scaling errors on the assumed uncertainties.

An alternative – albeit non-equivalent – way to test the presence of an orbital wobble in the data is to test whether the four Thiele-Innes constants are significantly different from 0. The first kind risk associated with the rejection of the null hypothesis ‘the orbital semi-major axis is equal to zero’ may be expressed as

$$Pr_3 = Pr(\chi_{ABFG}^2 < \chi_4^2), \quad (5)$$

where $\chi_{ABFG}^2 = \mathbf{X}^t \mathbf{C}^{-1} \mathbf{X}$, \mathbf{X} is the vector of components A, B, F, G and \mathbf{C} is its covariance matrix. Pr_3 is thus the probability that χ_4^2 , the χ^2 random variable with 4 degrees of freedom, exceeds the given value χ_{ABFG}^2 . The Pr_3 test, being based on the χ_{ABFG}^2 statistics, is an absolute test, and it is therefore sensitive to possible scaling errors on the assumed uncertainties.

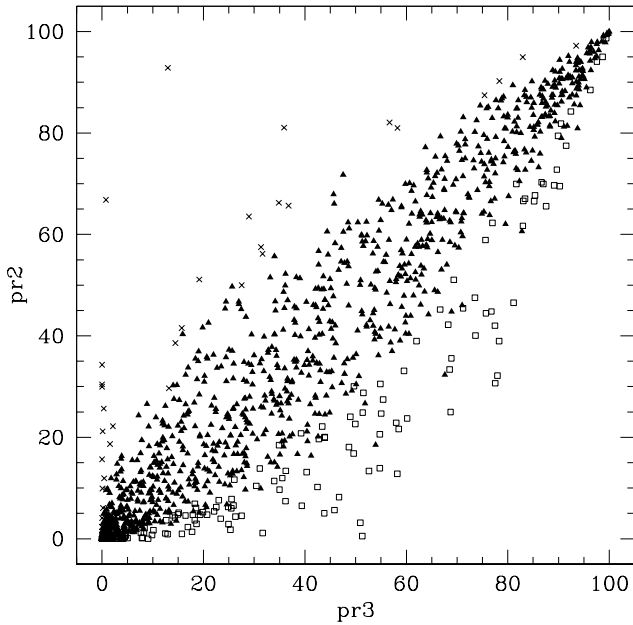


Fig. 3. Comparison of the Pr_2 and Pr_3 statistics for the whole sample of 1374 stars, showing that Pr_2 and Pr_3 are not equivalent. Crosses correspond to systems with $F2_{TI} > 2.37$, where $F2_{TI}$ is the goodness-of-fit for the Thiele-Innes model (Eq. 6); open squares correspond to systems with $F2_{TI} < -1.95$.

Because a_0 vanishes when there is no wobble present in the data (and conversely), it may seem that the Pr_2 and Pr_3 tests are equivalent (notwithstanding the fact that the former test is relative, whereas the latter is absolute). As revealed by Fig. 3, this is not necessarily so, though, for the reasons we now explain. Since the model is linear, the equality $\chi_T^2 = \chi_S^2 - \chi_{ABFG}^2$ holds. Therefore, $\hat{F} = \frac{n-9}{4} \frac{\chi_S^2 - \chi_T^2}{\chi_T^2} = \frac{n-9}{4} \frac{\chi_{ABFG}^2}{\chi_T^2}$, so that Pr_2 and Pr_3 are basically equivalent as long as $\chi_T^2 \sim n - 9$, i.e., when the Thiele-Innes model fits the data adequately. This latter fit may be quantified by the goodness-of-fit statistics $F2_{TI}$ (Stuart & Ord 1994; Kovalevsky & Seidelmann 2004), defined

as:

$$F2_{TI} = \left(\frac{9\nu}{2} \right)^{1/2} \left[\left(\frac{\chi_T^2}{\nu} \right)^{1/3} + \frac{2}{9\nu} - 1 \right], \quad (6)$$

where $\nu = n - 9$ is the number of degrees of freedom. If the Thiele-Innes model holds, we expect $F2_{TI}$ to be approximately normally distributed with zero mean and unity standard deviation.¹ Bad fits correspond to large $F2$ values, abnormally good fits to large negative values. Solutions with $F2 > 2.37$ should be discarded at the 5% threshold.

Fig. 4 compares $F2$ with Pr_3 and reveals that the two tests are not simple substitutes of one another: there are systems which fail at the Pr_3 test but comply with the $F2$ test and conversely. The situation becomes clearer when one realizes that the upper envelope corresponds to the condition $Pr_2 < 0.05$, which may be translated into a lower bound on χ_{ABFG}^2 / χ_T^2 : solutions retained by the Pr_2 test have large χ_{ABFG}^2 / χ_T^2 ratios. There are two ways to fulfill such a condition: If χ_T^2 is small (i.e., $F2$ is small, or abnormally good fits), then even small χ_{ABFG}^2 values (i.e., large Pr_3) comply with the Pr_2 test. This explains why the Pr_2 test does not eliminate systems with large Pr_3 when their Thiele-Innes fit is abnormally good. Conversely, if χ_{ABFG}^2 is large (i.e., Pr_3 is small), then even large χ_T^2 values (i.e., large $F2$ or bad Thiele-Innes fits) comply with the Pr_2 test. This explains why at small Pr_3 values, even bad Thiele-Innes fits (large $F2$ values) are retained. This would typically be the case of a DMSA/X system where the Thiele-Innes model brings a substantial improvement with respect to the single-star model (i.e., $\chi_{ABFG}^2 = \chi_S^2 - \chi_T^2$ is large, or Pr_3 is small), but the overall quality of the Thiele-Innes fit remains poor (large $F2$).

In the Campbell approach, the situation is somewhat more complicated since the model expressed by Eq. 1 does not depend linearly upon the model parameters i and Ω . Therefore, the quantity χ_C^2 extracted from the minimization of Eq. 1 does not follow a χ^2 distribution with $n - 2$ degrees of freedom (Lupton 1993). Since the non-linear model may be linearized at the expenses of adding more parameters (e.g., the coefficients of a Fourier or Taylor expansion), $n - 2$ overestimates the number of degrees of freedom (Pourbaix 2005). Overestimating the number of degrees of freedom affects all the statistical tests using the χ_C^2 value. In particular, the first kind risk Pr_1 extracted from an equation similar to Eq. 4 (substituting χ_T^2 by χ_C^2) is underestimated (Pourbaix 2005). Since this threshold is used to reject solutions which have Pr_1 larger than the adopted threshold, it may nevertheless be used, keeping in mind that not enough solutions are in fact discarded by the Pr_1 test. It is very likely, though, that these unacceptable solutions will be screened out by the other tests.

The combination of these four statistical indicators allows us to flag 282 stars as astrometric binaries at the 5% level (i.e.,

¹ The analysis of the single-star fits for the whole Hipparcos Catalogue reveals that the $F2$ statistics has a mean 0.21 and standard deviation 1.08 (ESA 1997). This indicates that the formal errors have been slightly underestimated. Since the same formal errors are used to compute χ_T^2 , the $F2$ statistics for the Thiele-Innes fits has been assumed to have the same parameters as for the single-star fits. Consequently, the 5% threshold corresponds to $F2 = 2.37$.

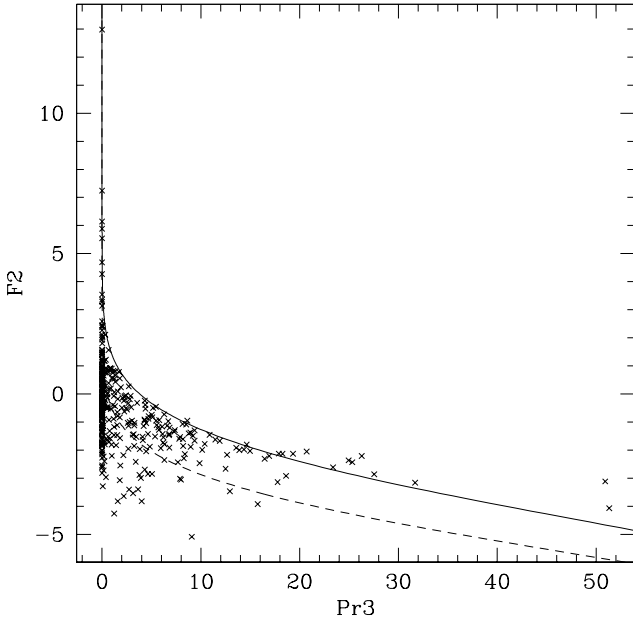


Fig. 4. $F2$ (goodness of fit) versus Pr_3 for systems complying with $Pr_2 < 5\%$. The envelope of these points is well reproduced with the theoretical curve (solid line) assuming $Pr_2 = 5\%$ and 59 observations (which corresponds to the average number of observations for the considered systems). The dashed line corresponds to $Pr_2 = 1\%$.

$Pr_1, Pr_2, Pr_3 < 0.05$ and $F2_{\text{TI}} < 2.37$) among the 1374 HIP+ S_{B9} sample stars defined in Sect. 3.

4.2. Detection rate

The 282 astrometric binary stars passing the four tests described in Sect. 4.1 at the 5% level are listed in Table 1. Italicized entries correspond to the 122 stars passing the Pr_1, Pr_2 and Pr_3 tests at the more stringent 0.006% level and $F2 < 2.37$. These stars thus represent prime targets for future astrometric observations or, if both components are visible, interferometric observations (see also Table 1A of Taylor et al. 2003), as they are astrometric binaries, but with orbital elements not always reliably determined (see Sect. 5).

We present the detection rate as a function of the parallax ϖ and the orbital period P in Table 2 and Figs. 5 and 6. A striking property of the astrometric-binary detection rate displayed in Fig. 5 is its increase around $P = 50$ d, due to the Hipparcos scanning law which does not favour the detection of shorter-period binaries. Similarly, the detection rate drops markedly for periods larger than 2000 d, corresponding to twice the duration of the Hipparcos mission. Worth noting are therefore the 5 astrometric orbits detected with periods larger than 5 000 d: HIP 116727 ($P = 24\,135$ d), HIP 5336 ($P = 8\,393$ d), HIP 7719 ($P = 7\,581$ d), HIP 11380 ($P = 6\,194$ d) and HIP 33420 ($P = 6\,007$ d). The reason why the astrometric motion of HIP 116727 could be detected despite such long an orbital period, is that Hipparcos caught it close to periastron

($e = 0.39$), when the orbital motion is the fastest. Table 2 further reveals that the detection rate exhibits little sensitivity to the parallax (provided it is larger than 5 mas; otherwise, the IAD are not precise enough to extract the orbital motion), but rather that it is the orbital period which plays the most significant role. The detection rate in the most favourable cases lies in the range 50 to 80%. It must be stressed, however, that *all the undetected astrometric binaries in those bins are either SB2 systems, systems with a composite spectrum or with a spectroscopic orbit of poor quality* (the SB2 and composite-spectrum systems have components of similar brightness, so that in most cases, the photocenter of the system does not differ much from its barycenter, making the orbital motion difficult to detect; see Eq. 8 below). If we remove these entries from the sample, the detection rate is close to 100%. The orbital parameters of the detected binaries are further analyzed in Sect. 5. Such an analysis is made necessary when one realizes that the orbital inclinations derived by the Thiele-Innes and Campbell approaches do not always yield consistent values (Fig. 7), contrary to expectations. Sect. 5 therefore presents further criteria used to evaluate the reliability of the derived astrometric orbital elements (and, in particular, the consistency between the two sets of orbital parameters, Thiele-Innes versus Campbell).

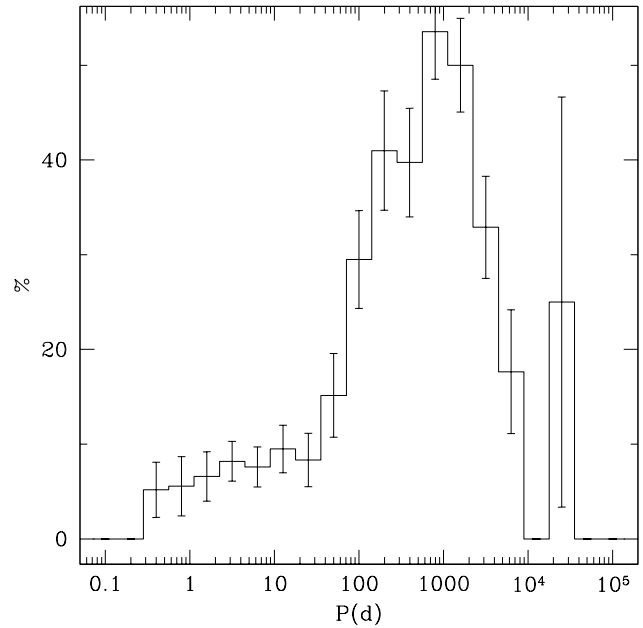


Fig. 5. Percentage of astrometric binaries detected among S_{B9} stars as a function of orbital period. The error bars give the binomial error on each bin.

4.3. The DMSA/O entries

Among the 1374 binaries from S_{B9} , 122 are flagged as DMSA/O in the Hipparcos catalogue. We detect 89 of these (or 75%) (irrespective of ϖ). The detection rate climbs to 81.7% (85/104) for orbital periods longer than 100 d. It is worth exam-

Table 1. The 282 stars flagged as astrometric binaries ($Pr_1, Pr_2, Pr_3 < 0.05$ and $F2_{\text{TI}} < 2.37$; see text). Italicized entries identify the 122 stars passing the Pr_1, Pr_2 and Pr_3 tests at the more stringent 0.006% level, and $F2_{\text{TI}} < 2.37$.

HIP	HIP	HIP	HIP	HIP	HIP	HIP	HIP	HIP	HIP	HIP	HIP	HIP
443	7564	<i>13055</i>	22961	<i>31681</i>	43346	<i>52419</i>	60292	<i>73440</i>	81170	92112	99089	<i>109176</i>
677	7719	14273	23402	32713	43413	52444	<i>60998</i>	<i>74087</i>	82706	92175	<i>99675</i>	109554
<i>1349</i>	8645	<i>15394</i>	<i>23453</i>	32761	43557	52650	<i>61724</i>	<i>75379</i>	<i>82860</i>	92177	<i>99848</i>	<i>110130</i>
<i>1955</i>	8903	15900	23743	<i>32768</i>	<i>43903</i>	52958	62437	<i>75695</i>	<i>83575</i>	<i>92512</i>	<i>99965</i>	110273
<i>2081</i>	8922	16369	23922	33420	44124	<i>53238</i>	<i>62915</i>	<i>75718</i>	83947	92614	100384	110514
2865	9110	17136	23983	<i>34164</i>	44455	<i>53240</i>	<i>63406</i>	76267	84677	<i>92872</i>	<i>100437</i>	111104
3300	9121	17296	<i>24419</i>	<i>34608</i>	<i>44946</i>	53425	63592	76574	84886	92818	100738	<i>111170</i>
3362	10340	<i>17440</i>	24984	35412	<i>45075</i>	53763	64422	76600	<i>84949</i>	<i>92872</i>	<i>101093</i>	111191
<i>3504</i>	<i>10514</i>	17683	25048	36042	45333	54632	<i>65417</i>	77409	85829	<i>93244</i>	101780	<i>112158</i>
3572	10644	17932	25776	<i>36377</i>	46005	<i>55016</i>	65522	77634	85985	<i>94371</i>	<i>101847</i>	<i>113718</i>
3951	<i>10723</i>	18782	<i>26001</i>	36429	46613	55022	67195	77678	<i>86400</i>	<i>95028</i>	102388	<i>113860</i>
4166	<i>11231</i>	19248	26291	37908	<i>46893</i>	<i>56731</i>	<i>67234</i>	77801	<i>86722</i>	<i>95066</i>	<i>103519</i>	<i>114313</i>
4252	<i>11349</i>	<i>20070</i>	<i>27246</i>	<i>38414</i>	47205	<i>57791</i>	<i>67480</i>	78689	<i>87895</i>	95176	<i>103722</i>	<i>114421</i>
4584	11380	<i>20087</i>	28537	39341	<i>47461</i>	58590	<i>67927</i>	<i>79101</i>	<i>88788</i>	<i>95575</i>	<i>103987</i>	<i>116478</i>
4754	11465	20284	29276	<i>39424</i>	49561	59148	<i>68072</i>	79195	88946	95820	105017	<i>116727</i>
4843	11843	20482	29740	<i>39893</i>	<i>49841</i>	59459	<i>68682</i>	<i>79358</i>	89773	95823	105432	<i>117229</i>
<i>5336</i>	<i>11923</i>	<i>20935</i>	29982	40240	50005	59468	<i>69112</i>	80042	<i>89808</i>	96467	105860	117317
<i>5881</i>	<i>12062</i>	<i>21123</i>	<i>30277</i>	<i>40326</i>	50801	59551	<i>69879</i>	80166	<i>89937</i>	97150	<i>105969</i>	117607
<i>6867</i>	12472	21433	30338	41784	50966	59609	69929	<i>80346</i>	<i>90098</i>	97446	106267	
<i>7078</i>	<i>12709</i>	21673	30501	42327	<i>51157</i>	59856	<i>72848</i>	<i>80686</i>	<i>90135</i>	97456	107136	
7145	12716	21727	<i>31205</i>	42542	<i>52085</i>	<i>60061</i>	72939	<i>80816</i>	<i>90659</i>	97594	108473	
7487	<i>12719</i>	22407	31646	42673	52271	60129	<i>73199</i>	<i>81023</i>	<i>91751</i>	98039	109067	

Table 2. Detection rate (expressed in %) as a function of orbital period and parallax. The percentage is given along with its binomial error; the total number of stars in the bin is listed between parentheses. For $\varpi > 5$ mas and $100 \leq P(\text{d}) \leq 3000$, the detection rate comes close to 100% when removing SB2 systems, systems with composite spectra or with a poor-quality spectroscopic orbit.

		Period range (d)				
		0–100	100–2 000	2 000–3 000	3 000–5 000	any P
Parallax (mas)	over 15	16±3 (177)	69±5 (81)	58±14 (12)	9±12 (12)	35±3 (292)
	10–15	7±2 (106)	69±7 (42)	80±18 (5)	18±19 (5)	26±3 (162)
	5–10	8±2 (232)	51±6 (74)	65±12 (17)	18±14 (5)	21±2 (336)
	0–5	7±1 (351)	24±3 (170)	4±4 (25)	5±5 (21)	12±1 (584)
	any ϖ	9±1 (866)	45±3 (367)	39±6 (59)	28±7 (43)	21±1 (1 374)

ining why not all DMSA/O solutions were retrieved by our processing. A close look at the rejected systems reveals that there is nothing wrong with our analysis, since all but one among the 33 DMSA/O systems not recovered by our reprocessing belong to one of the following categories:

- the star is in fact SB2 and possesses an astrometric orbit obtained from ground-based interferometric or speckle observations; for those cases, the DMSA/O solution only provides a_0 , with all other parameters taken from the ground-based astrometric solution (HIP 2912, HIP 10064, HIP 13531, HIP 14328, HIP 14576, HIP 24608, HIP 28360, HIP 55266, HIP 57565, HIP 96683, HIP 105431);
- as indicated in a DMSA/O note, the orbital solution is in fact of poor quality (‘Spectroscopic orbit unreliable. Probably single’ *sic*), and does not comply with our more stringent tests (HIP 10366, HIP 24727, HIP 26563, HIP 35550, HIP 45527);
- more orbital elements have been imposed than done here (e.g., the inclination, from the eclipsing nature of the star: HIP 100345; also HIP 23416 = ϵ Aur);
- the period provided by the DMSA/O solution is totally different from the one listed in S_{B9} (HIP 8882, HIP 17847, HIP 63613, HIP 82020, HIP 91009 = BY Dra), sometimes because the system is a triple one (HIP 85333, HIP 100345);
- the solution has been marginally rejected by our tests, i.e., Pr_1, Pr_2 or Pr_3 are only slightly larger than 5% (HIP 5778, HIP 32578, HIP 68756) or $F2$ is slightly larger than 2.37 (HIP 8833, HIP 59750), or similarly, the DMSA/O solution is of too low a quality to comply with the tests devised in the present paper (HIP 10324, HIP 12623, HIP 21273).

HIP 85749 is the only DMSA/O solution not belonging to any of the above categories. HIP 85749 has not been flagged

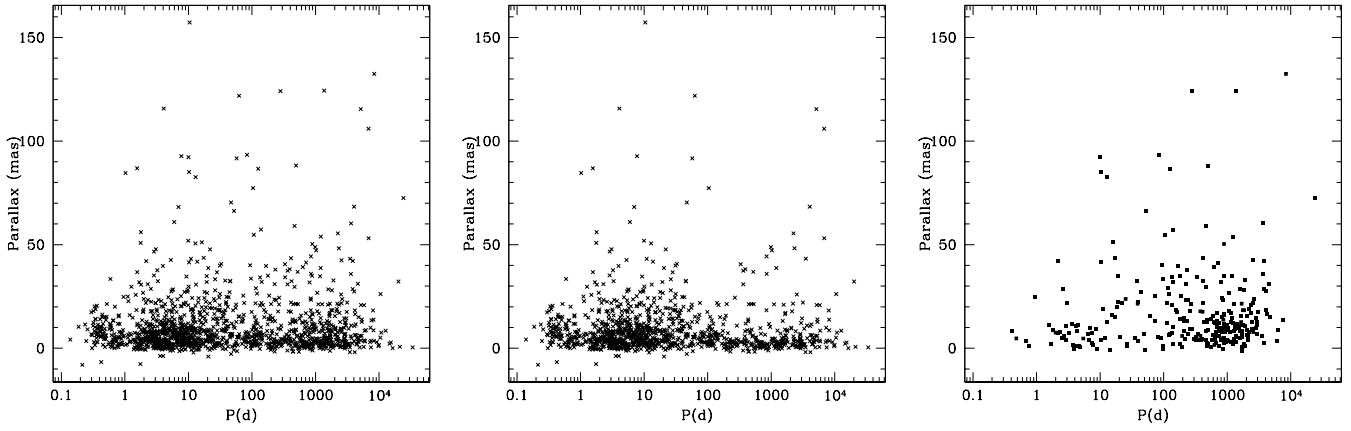


Fig. 6. **Left panel:** Period-parallax diagram for the selected S_{B9} objects with an HIP entry. **Middle panel:** Period-parallax diagram for non-detected objects. **Right panel:** Stars flagged as astrometric binaries by the Pr_1 , Pr_2 and Pr_3 tests at the 5% level and with $F2_{TI} < 2.37$.

as an astrometric binary by our reprocessing, because $Pr_1 = 0.26$, although Pr_2 , Pr_3 and $F2$ do qualify the star as an astrometric binary.

5. Orbit assessment

The upper panel of Fig. 7 reveals that, even though orbital solutions pass the Pr_1 , Pr_2 and Pr_3 tests, meaning that an astrometric orbital motion has been detected, these solutions do not necessarily yield Thiele-Innes and Campbell orbital elements that are consistent with each other. The inverse-S shape observed in Fig. 7 results from the following properties: (i) in the absence of an orbital signal in the IAD and when the spectroscopic radial-velocity semi-amplitude K_1 is small, the Campbell solution tends to have $i_C \sim 0^\circ$ or 180° , while the Thiele-Innes solution tends to $i_{TI} \sim 90^\circ$ (Pourbaix 2004); (ii) the physical solutions fall on the diagonal, although this diagonal is polluted with unphysical solutions having $i_{TI} \sim 90^\circ$. The lower panel of Fig. 7 displays the 122 stars complying with the Pr_1 , Pr_2 and Pr_3 tests at the 0.006% level. It clearly shows that the consistency between the Thiele-Innes and Campbell solutions may be improved considerably by decreasing the probability threshold to 0.006%.

To remove the remaining inconsistent solutions, it is necessary to assess the reliability of the derived orbital elements. This may be done in at least two ways:

- The consistency between the Thiele-Innes and Campbell elements could be checked directly by computing error ellipsoids around the two sets of orbital elements and estimating whether or not they intersect. This method has not been applied here, because it is very time-consuming.
- Empirical tests have been devised which check that (i) the astrometric orbital signal has the same period as the adopted spectroscopic period; (ii) the astrometric orbital elements should not be too much correlated with each other. This test was already used by Pourbaix & Boffin (2003) in a similar context.

The empirical approach has been preferred here, with the two tests involved now described in turn.

First, the consistency between the astrometric period and the adopted spectroscopic period is checked through a periodogram-like test. For 600 periods uniformly distributed in $\log P$ between 0.1 and 1200 d, the best 9-parameter (Thiele-Innes) fit is computed (the eccentricity and periastron time are kept unchanged). The resulting χ^2 is plotted against the period, thus generating a Scargle-like periodogram (Scargle 1982). Its standard deviation σ is computed. An orbital motion with the expected (spectroscopic) period is then supposed to be present in the IAD if the χ^2 at that period is smaller than the periodogram mean value by more than $\xi\sigma$, with ξ chosen of the order of 3.

Second, the correlation existing between the Thiele-Innes orbital elements may be estimated through the *efficiency* parameter ϵ (Eichhorn 1989), expressed by

$$\epsilon = \sqrt[p]{\frac{\prod_{k=1}^p \lambda_k}{\prod_{k=1}^p \mathbf{V}_{kk}}}, \quad (7)$$

where λ_k and \mathbf{V}_{kk} are respectively the eigenvalues and the diagonal terms of the covariance matrix \mathbf{V} and p denotes the number of parameters in the model. For an orbital solution to be reliable, its covariance matrix should be dominated by the diagonal terms, and the *efficiency* ϵ should then be close to 1 (Eichhorn 1989).

The 70 orbital solutions retained when adopting $\xi = 3$ and $\epsilon > 0.4$ are listed in Table 3, 20 of them being new orbital solutions not already listed in the DMSA/O annex. Fig. 8 presents the distribution of their orbital periods. In Fig. 9 comparing the inclinations derived from the Thiele-Innes and Campbell solutions, the retained orbits now fall close to the diagonal, as expected.

Neither the parallax nor the proper motions differ significantly from the Hipparcos value for the stars of Table 3. They have therefore not been listed.

To increase the science content of this paper, Table 4 lists the astrometric orbital elements for a second category of sys-

Table 3. The 70 orbital solutions (Campbell solutions) passing all consistency tests. The column labelled ‘Ref.’ provides the reference for the spectroscopic orbit used. In the case where a system is listed in the DMSA/O annex, the column labelled ‘DMSA’ compares the orbital semi-major axes and the inclinations from the DMSA/O annex and from this work.

HIP	a_0 (mas)	e	i (°)	ω_1 (°)	Ω (°)	T_0 (JD - 2 400 000)	P (d)	DMSA (a/a_{hip} ; i/i_{hip})	Ref.
677	7.26±0.38	0.53	102.7±9.7	77.5	103.4±5.8	47374.6	96.7	O(1.12;0.97)	Pourbaix (2000)
1349	20.98±0.56	0.57	74.7±2.1	4.7	352.3±3.3	34233.3	411.4	O(1.05;0.93)	Bopp et al. (1970)
1955	4.68±0.25	0.33	108.0±7.5	18.7	299.0±8.3	35627.6	115.3	5	Barker et al. (1967)
3504	7.4±1.3	0.11	107.2±4.3	79.0	274.5±4.7	41665.0	1033.0	O(1.04;1.06)	Abt & Levy (1978)
6867	5.57±0.46	0.00	46.3±4.0	0.0	340.2±5.2	19544.9	193.8	O(1.13;0.92)	Luyten (1936)
7078	7.95±0.15	0.31	85.6±4.7	188.2	160.5±3.7	29000.4	134.1	O(1.28;0.97)	Wright & Pugh (1954)
8903	12.5±1.2	0.88	44.7±5.0	24.9	77.8±5.6	44809.1	107.0	O(1.10;1.00)	Pourbaix (2000)
8922	8.14±0.93	0.00	23.6±1.8	0.0	155.7±4.1	43521.5	838.0	X	Griffin (1981b)
10514	5.1±1.4	0.06	68±11	63.0	318±14	41981.5	1385.0	O(0.95;0.92)	Griffin & Radford (1977)
11231	8.09±0.34	0.29	60.6±3.7	188.2	200.2±3.8	37159.1	142.3	O(1.43;2.43)	Barker et al. (1967)
12062	10.99±0.87	0.26	56.8±4.0	254.6	64.9±5.8	46440.0	905.0	X	Latham et al. (2002)
20935	11.5±1.1	0.24	16.5±1.3	127.0	308.3±3.5	43298.5	238.9	O(1.06;0.83)	Griffin et al. (1985)
24419	10.77±0.59	0.08	51.6±3.3	275.0	230.7±3.9	50690.0	803.5	9	Nidever et al. (2002)
26001	5.55±0.46	0.51	52.2±5.2	330.0	45.4±6.6	23108.4	180.9	O(1.21;1.17)	Lunt (1924)
30277	9.02±0.52	0.70	116.3±4.2	117.1	294.6±5.0	19915.0	868.8	O(0.94;1.01)	Spencer Jones (1928b)
32768	7.15±0.25	0.09	80.2±6.1	64.0	2.9±6.2	20992.8	1066.0	O(0.90;1.00)	Spencer Jones (1928a)
34164	8.77±0.96	0.27	107.4±8.5	248.9	224.3±8.0	47859.9	612.3	X	Latham et al. (2002)
34608	4.92±0.31	0.40	64.3±5.9	103.4	85.6±6.9	44525.0	113.3	O(1.16;0.72)	Beavers & Salzer (1985)
36377	8.32±0.32	0.17	65.6±3.3	349.3	0.0±5.2	20418.6	257.8	O(1.02;0.96)	Wilson (1918)
39893	9.9±1.3	0.21	155.3±2.2	210.0	193.1±6.6	48342.0	733.5	X	Latham et al. (2002)
40326	10.66±0.73	0.40	135.2±1.9	140.0	181.7±2.7	18060.0	930.0	O(0.98;0.99)	Christie (1936)
45075	10.35±0.42	0.48	61.3±3.2	349.4	119.2±3.8	25721.6	1062.4	O(0.92;0.91)	Bretz (1961)
47461	4.19±0.67	0.15	122.0±8.0	135.4	282.7±9.7	45464.5	635.4	5	Ginestet et al. (1991)
52085	8.09±0.62	0.10	125.0±4.4	270.0	327.5±6.9	20760.0	1200.0	O(1.36;0.85)	Christie (1936)
53240	7.83±0.93	0.38	134.4±5.4	301.0	292.4±6.2	42901.5	1166.0	O(0.90;1.09)	Griffin (1980)
57791	7.47±0.60	0.31	86.5±6.1	125.1	108.5±4.8	42352.7	486.7	O(0.97;0.99)	Ginestet et al. (1985)
60998	5.99±0.93	0.30	32.5±4.4	244.0	205.7±8.6	42868.0	1703.0	7	Reimers et al. (1988)
61724	8.40±0.82	0.59	81.5±6.8	102.5	139.0±7.0	43304.0	972.4	O(0.84;0.96)	Griffin (1981a)
62915	5.35±0.76	0.32	27.1±3.3	194.0	40.7±8.4	43424.5	1027.	9	Griffin (1983)
63406	14.12±0.47	0.33	81.8±5.0	65.0	101.3±4.9	49220.0	710.6	O(0.86;1.01)	Griffin (2002b)
65417	12.0±1.7	0.19	68.9±4.6	166.0	121.1±3.7	45497.5	1366.8	O(1.17;1.13)	Griffin (1986)
67234	6.45±0.61	0.13	48.2±3.8	58.6	280.3±4.9	24163.0	437.0	O(1.01;0.77)	Spencer Jones (1928b)
67927	36.02±0.56	0.26	115.7±1.6	326.3	75.2±1.4	28136.2	494.2	O(1.02;0.99)	Bertiau (1957)
67480	7.3±0.9	0.41	174.0±0.5	359	278.8±5.8	44739.5	944	X	Griffin (1985)
69112	5.74±0.55	0.14	130.2±3.8	311.8	158.5±5.3	38901.7	605.8	O(1.00;0.94)	Scarfe (1971)
69879	4.65±0.24	0.57	89.8±9.1	224.9	347.0±8.6	40286.0	212.1	O(1.26;1.02)	Scarfe & Alers (1975)
72848	16.54±0.18	0.51	93.4±4.2	219.0	248.3±3.6	50203.4	125.4	O(1.16;0.94)	Nidever et al. (2002)
73199	6.10±0.48	0.13	53.3±4.0	212.0	239.3±5.5	44419.0	748.9	O(0.85;0.84)	Batten & Fletcher (1986)
73440	4.69±0.47	0.22	43.9±5.2	10.0	288.5±6.5	47349.0	467.2	X	Latham et al. (2002)
74087	11.2±1.6	0.83	62.0±9.0	175.3	82.6±6.6	48356.6	2567.1	7	Griffin & Eitter (1999)
75379	8.4±1.3	0.68	52.6±9.4	339.5	215.5±7.5	14785.1	226.9	O(1.00;1.07)	Jones (1931)
79101	8.65±0.64	0.47	10.3±0.7	357.0	148.3±3.0	40525.2	560.5	O	Aikman (1976)
80346	53.0±1.8	0.67	152.60±0.95	251.0	286.9±1.5	51298.0	1366.1	O(1.02;1.03)	Nidever et al. (2002)
80686	2.71±0.44	0.06	16.01±2.47	274.5	2.1±6.8	18103.6	12.9	5	Spencer Jones (1928b)
80816	11.37±0.51	0.55	53.8±2.3	24.6	341.9±3.8	15500.4	410.6	O(1.03;1.16)	Plummer (1908)

Table 3. Continued.

HIP	a_0 (mas)	e	i ($^\circ$)	ω_1 ($^\circ$)	Ω ($^\circ$)	T_0 (JD - 2 400 000)	P (d)	DMSA (a/a_{hip} ; i/i_{hip})	Ref.
82860	6.58±0.32	0.21	56.1±4.0	339.0	228.7±4.5	39983.6	52.1	O(0.98;0.90)	Abt & Levy (1976)
83575	9.11±0.58	0.22	61.2±3.5	348.0	19.5±4.3	46806.0	790.6	O(1.04;1.03)	Griffin (1991)
86400	12.71±0.78	0.23	18.4±1.1	140.5	274.2±2.7	47724.9	83.7	O(0.92;0.41)	Tokovinin (1991)
87895	29.81±0.62	0.41	72.7±1.2	134.8	177.4±1.0	47714.6	881.8	O(1.09;1.07)	Pourbaix (2000)
88788	10.09± 1.04	0.378	153.9± 2.3	137.0	341.4±5.8	46139.0	2017.0	9	Griffin (1992)
89937	50.30±0.23	0.41	80.08±0.70	119.9	232.42±0.83	46005.6	280.5	O(1.25;1.07)	Pourbaix (2000)
90659	9.1±1.1	0.50	142.1±3.0	56.0	353.1±6.0	42925.5	1284.0	O(0.97;1.01)	Griffin (1980)
91751	6.41±0.53	0.21	59.5±4.9	78.0	295.8±7.0	42928.5	485.3	O(1.05;1.05)	Griffin (1982b)
92512	3.16±0.25	0.11	106±11	274.3	0±37	19258.2	138.4	O(1.02;1.09)	Young (1920)
93244	12.80±0.44	0.27	87.5±6.6	82.0	58.7±3.9	41718.5	1270.6	O(0.94;1.00)	Griffin (1982b)
95028	3.0 ± 0.7	0.37	19 ± 4	161	242.9 ± 10.0	43811.9	208.8	7	Griffin (1982b)
95066	9.15±0.54	0.83	75.2±8.6	152.7	129.7±6.7	33420.2	266.5	O(1.18-1.05)	Franklin (1952)
95575	8.14±0.25	0.15	98.2±7.8	63.3	208.1±5.7	47746.4	166.4	X	Tokovinin (1991)
99848	5.5±1.2	0.30	65.5±8.3	218.2	0±227	33141.8	1147.8	O(1.04;1.02)	Wright (1970)
99965	14.06±0.39	0.08	92.2±3.6	243.0	303.9±4.5	50218.0	418.8	O(0.87;0.94)	Griffin (2002a)
100437	5.35±0.57	0.76	54.2±6.4	108.1	249.7±8.2	49281.0	1124.1	9	Griffin & Eitter (2000)
101093	19.79±0.55	0.03	104.0±1.6	83.7	95.4±1.7	16214.5	840.6	O(1.39;1.01)	Abt (1961)
101847	3.82± 0.81	0.0	147.7± 5.9	0.0	314.0±1.3	23358.0	205.2	5	Lucy & Sweeney (1971)
103519	7.48±0.64	0.44	32.4±2.4	148.1	306.2±4.0	39186.1	635.1	O(1.02;0.94)	Radford & Griffin (1975)
105969	10.65±0.75	0.13	157.0±1.3	192.0	236.6±3.9	47479.0	878.0	X	McClure (1997)
109176	4.07±0.27	0.00	80±13	0.0	188±11	45320.0	10.2	5	Fekel & Tomkin (1983)
111170	26.67±0.73	0.38	63.4±1.7	171.6	82.0±1.9	43995.0	630.1	O(1.14;1.07)	Pourbaix (2000)
112158	15.62±0.85	0.15	72.7±1.9	5.6	208.6±2.3	15288.7	818.0	O(1.15;1.03)	Crawford (1901)
113718	12.16±0.93	0.54	24.3±1.8	247.7	328.6±5.6	48280.0	468.1	O(1.10;0.41)	Latham et al. (2002)
114421	7.82± 0.47	0.66	114.3±5.2	240.8	120.8±7.2	16115.6	409.6	O(1.26;0.93)	Spencer Jones (1928b)

tems: 31 newly derived orbits (*i.e.*, not already present in the DMSA/O annex), not already listed in Table 3, from the list of 122 stars passing the Pr_1 , Pr_2 and Pr_3 tests at the 0.006% level (they are among the italicized stars in Table 1). These orbits are (possibly) of a slightly lower accuracy as the ones listed in Table 3 because they do not comply with the two empirical tests described in this section. Nevertheless, these newly derived orbits are worth publishing.

As already discussed in Sect. 4.3, there are 122 systems in our sample of 1 374 which have a DMSA/O entry. Of these 122, 89 pass the Pr_1 , Pr_2 , Pr_3 and $F2$ tests at the 5% level (Sect. 4.3) and 71 pass the Pr_1 , Pr_2 , Pr_3 and $F2$ tests at the 0.006% level but only 50 have reliable orbital elements according to the 2 empirical tests described in this section. The 39 rejected DMSA/O systems are listed in Table 5, along with the failed test(s). Fig. 10 compares the Thiele-Innes and Campbell inclinations for those systems with orbital elements not validated by the consistency tests.

The orbits derived in the present analysis and the DMSA/O ones generally agree well. For HIP 677 (= α And), a visual and SB2 system, there are astrometric orbits based on ground-based interferometric measurements already available (Pan et al. 1992; Pourbaix 2000). The inclination of $103^\circ \pm 10^\circ$ found here is consistent with the value $105.7^\circ \pm 0.2^\circ$ ob-

tained by Pan et al. (1992). The only new constraint of interest provided by the IAD-derived photocentric orbit lies in a consistency check between that photocentric semi-major axis $a_0 = 7.3 \pm 0.4$ mas (Table 3) and the relative semi-major axis $a = 24.1 \pm 0.1$ mas (Pan et al. 1992; Pourbaix 2000), with the following relation to be satisfied (Binnendijk 1960):

$$a_0 = a(\kappa - \beta), \quad (8)$$

where $\kappa = M_2/(M_1 + M_2) = 0.331$ and $\beta = (1 + 10^{0.4\Delta m})^{-1}$, and Δm is the magnitude difference between the two components. Eq. 8 then implies $\beta = 0.027$ or $\Delta m = 3.9$ mag, which is much larger than the value of 2.0 mag measured by Pan et al. (1992) or 2.19 mag derived by Ryabchikova et al. (1999). With $\Delta m = 2$ mag, $\beta = 0.137$, so that $a_0/a = 0.19$ or $a_0 = 4.7$ mas, which is inconsistent with the value of 7.3 ± 0.4 mas listed in Table 3 or $a_0 = 6.47 \pm 1.16$ mas from the DMSA/O. The origin of this discrepancy is unknown.

In Table 5, cases where the efficiency test is the only one to fail generally correspond to rather wide orbits which cannot be accurately determined with Hipparcos data only (*e.g.*, HIP 5336, 68682, 75695, 110130). When only the periodogram test fails, it means that either the spectroscopic period does not

Table 4. The 31 new orbital solutions (Campbell solutions) passing the Pr_1 , Pr_2 and Pr_3 tests at the 0.006% level, but failing at least one of the consistency tests. The column labelled ‘Ref.’ provides the reference for the spectroscopic orbit used. The columns labelled ξ and ϵ provide the values of the corresponding empirical tests. The column labelled ‘D’ refers to DMSA.

HIP	a_0 (mas)	e	i ($^\circ$)	ω_1 ($^\circ$)	Ω ($^\circ$)	T_0 (JD - 2 400 000)	P (d)	D	ξ	ϵ	Ref.
2081	103.5±8.2	0.34	128.0±5.4	19.8	242.8 ± 3.9	16201.8	3848.8	7	4.25	0.01	Lunt (1924)
5881	7.7±1.6	0.12	157.2±4.1	313	236.8± 8.1	51791.1	701.4	5	1.91	0.42	Nidever et al. (2002)
11349	84.4±4.5	0.01	115.8±5.0	225.	44.4± 8.2	45901.	3600.	9	3.31	0.07	Latham et al. (2002)
11923	33±32	0.54	86.2±24.6	259.0	83± 20	47774.2	2332.	7	4.39	0.07	Latham et al. (2002)
13055	8.12±0.77	0.09	85.0±13.7	120	279± 16	46344	2018	7	4.41	0.34	McClure & Woodsworth (1990)
15394	21.9±3.0	0.86	137.2±5.9	71.7	81± 10	51190.3	3089.4	7	2.18	0.11	Latham et al. (2002)
27246	56.3±6.8	0.32	49.6±7.2	318.5	344.6± 4.4	49649.	4072.	9	5.11	0.02	Latham et al. (2002)
31681	78.7±2.3	0.89	106.7±1.7	312.6	243.6± 2.6	43999.1	4614.5	X	2.61	0.01	Lehmann et al. (2002)
38414	32.7±2.2	0.38	41.3±1.9	170.	148.5± 3.6	17031.	2554.0	9	5.17	0.10	Parsons (1983)
39424	19.5±2.9	0.06	50.8±8.4	264.	242.6± 5.5	42894.5	2437.8	7	2.78	0.11	Griffin (1982a)
43903	37±3422	0.70	84±33	194.1	184± 21	49093.7	1898.7	7	5.67	0.05	Carney et al. (2001)
44946	10.5±1.7	0.06	144.1±4.9	301.1	282.0± 9.7	28876.8	1700.7	7	2.88	0.28	Jackson et al. (1957)
46893	4.69±0.77	0.15	132.3±6.8	261.	2± 11	43119.5	830.4	X	2.84	0.86	Griffin (1981b)
51157	17.9±1.2	0.86	122.4±5.2	296.1	255.7± 5.5	44583.0	1180.6	9	2.78	0.41	Griffin (1987)
53238	29.6±5.0	0.16	143.5±5.3	285.	221.2± 7.0	45781.	1841.	7	2.73	0.21	Latham et al. (2002)
55016	19.0±3.1	0.41	53.6±7.3	336.5	287± 10	42054.	2962.7	7	3.00	0.15	Wolff (1974)
60061	19.6±2.7	0.41	51.3±7.7	302.6	11.8± 8.2	50134.	2167.	7	3.33	0.28	Latham et al. (2002)
68072	10.8±2.7	0.68	20.9±4.1	177.6	6± 10	47179.1	1620.3	7	4.43	0.32	Latham et al. (2002)
75718	38.6±1.0	0.97	60.3±1.8	253.9	95.8± 3.5	47967.5	889.6	7	3.20	0.29	Duquennoy et al. (1992)
79358	16.5±2.3	0.6	46.4±3.5	340.	305.4± 6.7	24290.	2150.	7	4.73	0.18	Christie (1936)
84949	24.0±1.1	0.67	70.2±3.2	40.0	150.4± 2.1	44545.8	2018.8	X	4.31	0.30	Scarfe et al. (1994)
86722	49.4±8.5	0.93	41.6±7.6	129.6	315± 11	49422.5	2558.4	7	3.50	0.01	Duquennoy et al. (1996)
90098	30.7±4.1	0.26	56.0±7.0	187.2	54.6± 8.4	18076.2	2214.	9	3.23	0.06	Spencer Jones (1928b)
90135	21.6±1.9	0.10	89±16.5	242.1	226± 14	18278.3	2373.7	7	2.85	0.13	Grobben & Michaelis (1969)
92872	26.6±3.4	0.24	31.9±3.6	35.	12.6± 7.7	44276.5	2994.	7	3.53	0.04	Griffin (1981b)
94371	33.9±3.8	0.19	135.5±5.4	103.	126.9± 6.1	41044.5	2561.	7	3.52	0.09	Griffin (1979)
103987	10.7±2.7	0.08	162.1±2.3	83.	15.6± 3.9	46639.0	377.8	9	2.34	0.23	Latham et al. (1992)
114313	17.2±2.2	0.22	20.2±1.9	237.	75.1± 4.8	46444.	1132.	9	3.31	0.38	Latham et al. (2002)
116478	20.9±1.1	0.33	109.8±6.8	304.3	129.1± 7.8	47403.	1810.	9	4.60	0.16	Latham et al. (2002)
116727	376±23189	0.38	86±47	166.0	16± 19	48625	24135	7	5.56	0.01	Griffin et al. (2002)
117229	9.38±0.78	0.52	102±12	192.3	251.7± 8.4	48425.8	1756.0	7	2.93	0.59	Latham et al. (2002)

correspond to the astrometric motion, or that the IAD do not constrain its period well enough.

6. Some astrophysical implications

6.1. Masses

Masses of the components of spectroscopic binaries with one visible spectrum (SB1) are encapsulated in the mass function

$$f(M_1, M_2) \equiv \frac{M_2^3 \sin^3 i}{(M_1 + M_2)^2} \equiv Q \sin^3 i, \quad (9)$$

where M_1 and M_2 are the masses of the primary and secondary components, respectively. The knowledge of the inclination as given in Table 3 gives directly access to the generalized mass

ratio Q listed in Table 6. To go one step further and have access to the masses themselves, supplementary information must be injected in the process. For main-sequence stars, this may come from the mass – luminosity relationship. The mass of the main-sequence primary component is estimated directly from its Hipparcos $B - V$ color index, converted into an absolute magnitude M_V using Table 15.7 of Cox (2000), and then into masses using Table 19.18 of Cox (2000). The corresponding masses are listed in Table 6. The major uncertainty on M_2 comes from the uncertainty on M_1 rather than from i . To fix the ideas, an uncertainty of 0.1 mag on $B - V$ translates into an uncertainty of 0.2 (or 0.1, 0.05) M_\odot on M_1 , and of 0.045 (0.032, 0.027) M_\odot on M_2 for $0 \leq M_V < 4$ (or $4 \leq M_V < 6$, $6 \leq M_V$, respectively). The position of stars from Table 3 on the main sequence has been checked from the Hertzsprung-

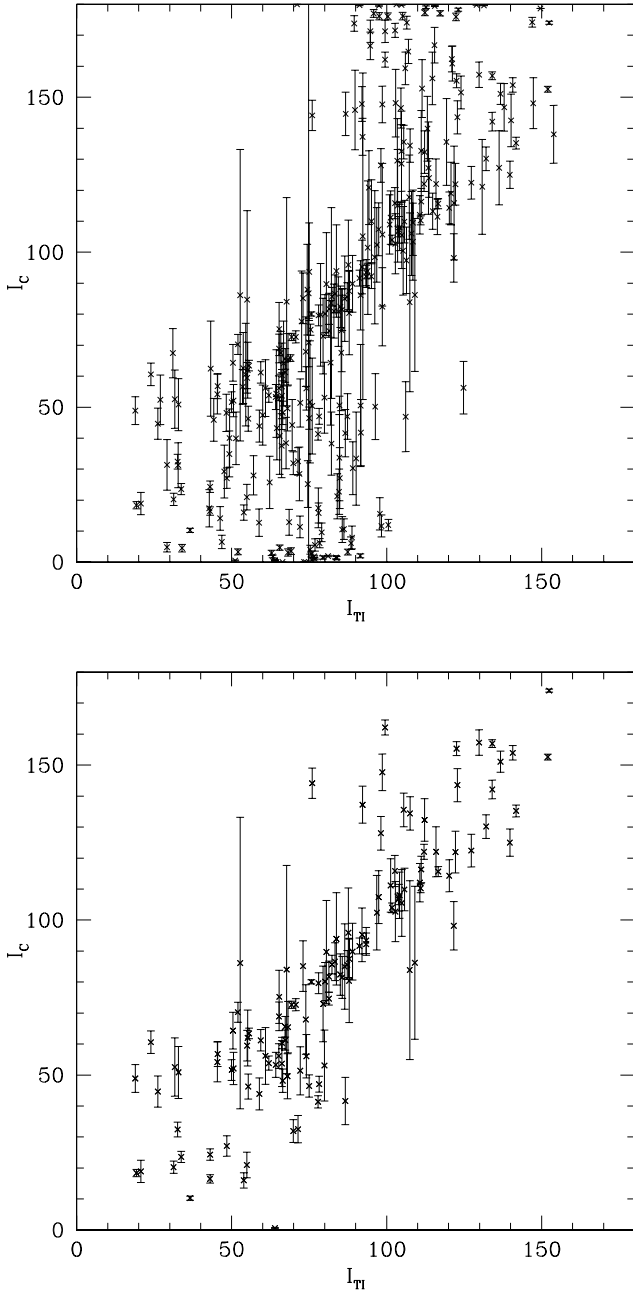


Fig. 7. Comparison of the orbital inclinations derived by the Thiele-Innes and Campbell approaches. The 282 stars displayed in the upper panel all comply with the 4 criteria for astrometric wobble detection (namely Pr_1, Pr_2 and $Pr_3 < 0.05$ and $F2_{TI} < 2.37$; see text), but their astrometric orbital elements are not always reliably determined as not all points fall along the diagonal. The lower panel displays the 122 stars complying with the Pr_1, Pr_2 and Pr_3 tests at the 0.006% level.

Russell diagram drawn from the Hipparcos data. In particular, it has been checked that the $B - V$ color is not the composite of the two components (in which case, the above procedure to derive M_1 may not be applied). Only HIP 47461 (= HD 83270) belongs to that category (as confirmed by Ginestet et al. 1991), so that neither masses are given in Table 6.

Table 5. The 39 systems with a DMSA/O entry which do not fulfill the 2 tests assessing the reliability of the astrometric orbital elements, namely $\xi < 3$ and $\epsilon > 0.4$ and the probability tests at the 0.006% level (see text). Columns with ‘n’ correspond to failed tests.

HIP	ξ	ϵ	Pr	Rem.
443	y	y	n	
5336	y	n	y	
10644	y	y	n	
10723	n	y	y	
12709	y	n	y	
12719	n	y	y	test failing only marginally
16369	n	y	n	
17296	n	y	n	
17440	y	n	y	
17932	y	y	n	
20070	n	y	y	
20087	n	n	y	DMSA/O solution provides only a_0
20482	n	y	n	
21123	n	y	y	
23453	n	y	y	test failing only marginally
23922	n	n	n	tests failing only marginally; DMSA/O solution from scratch providing a period different from the S_{B^9} one
29982	n	n	y	
30501	n	y	n	
31205	n	y	y	test failing only marginally
32761	y	y	n	test failing only marginally
49841	y	n	y	
52419	n	y	n	DMSA/O solution from scratch providing a period different from the S_{B^9} one
56731	y	n	y	test failing only marginally
58590	n	y	n	
59459	n	y	n	test failing only marginally
59468	y	y	n	
59856	n	n	n	test failing only marginally
68682	y	n	y	
75695	y	n	y	
76267	n	y	n	
80166	n	y	n	tests failing only marginally
81023	n	y	y	
89808	n	y	y	
92175	n	y	n	test failing only marginally
92818	y	y	n	test failing only marginally
99675	y	n	y	
109554	n	y	n	test failing only marginally
110130	y	n	y	
113860	y	n	y	

Individual systems of interest are discussed in Sect. 6.1.1.

The distributions of M_1 , M_2 and $q = M_2/M_1$ for the 29 systems with main sequence primaries are displayed in Fig. 11. The q distribution appears to be strongly peaked around $q = 0.6$, but this feature very likely results from the combination of two opposite selection biases. Our sample is biased against systems with $q \sim 1$ (since these systems would gener-

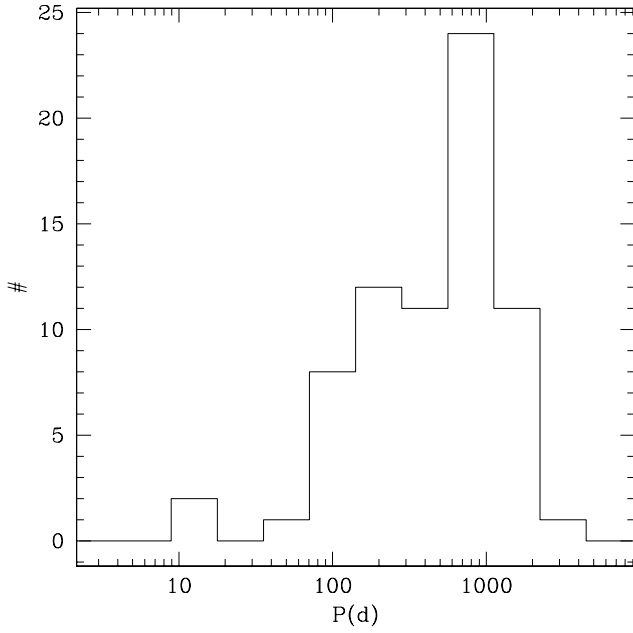


Fig. 8. Distribution of the orbital periods for the 70 solutions retained.

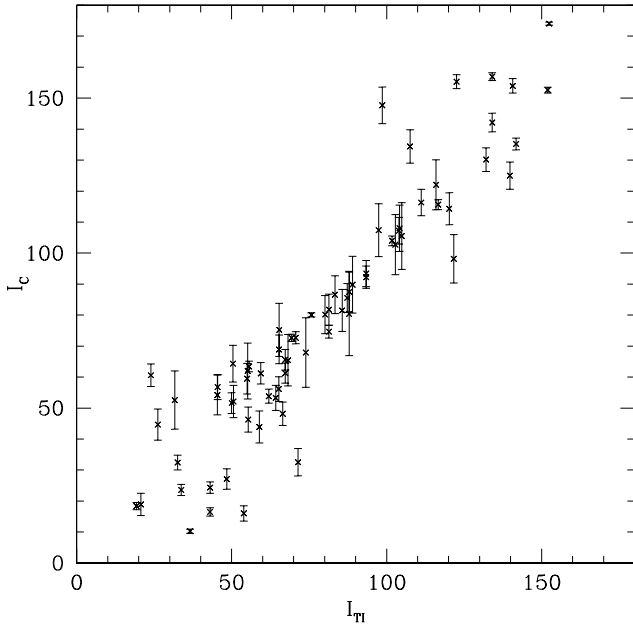


Fig. 9. Comparison of the inclinations derived from the Thiele-Innes constants and from the Campbell elements for the 70 systems retained. Compare with Fig. 7.

ally be SB2 systems with components of almost equal brightness, whose astrometric motion is difficult to detect; see the discussion of Sect. 4.2) and against systems with low-mass companions (which induce radial-velocity variations of small amplitude, difficult to detect, and thus not present in S_{B9}).

The M_1 and M_2 distributions also clearly reflect the bias against $q = 1$ since the distributions exhibit adjacent peaks.

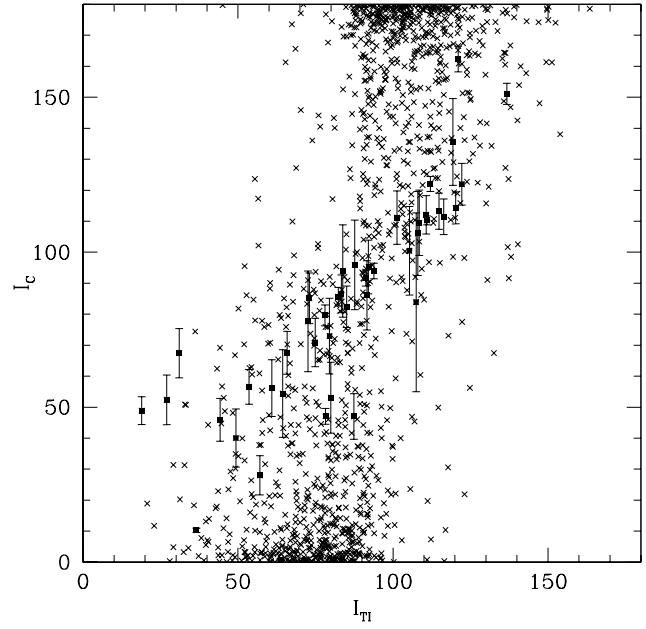


Fig. 10. Comparison of the inclinations derived from the Thiele-Innes constants and from the Campbell elements for the 1304 systems not retained. The 39 rejected systems with a solution in the DMSA/O annex (Table 5) are represented by a filled square.

Although one would be tempted to attribute the $M_2 = 0.6 M_\odot$ peak to a population of white dwarf (WD) companions, it is more likely to result from the two selection biases described above.

In the absence of a mass – luminosity relationship for giants, the mass of the companion cannot be derived reliably.

6.1.1. Masses for some specific systems

HIP 677 = α And

As already discussed in Sect. 5, HIP 677 is known to be a SB2 and visual binary (Ryabchikova et al. 1999; Pourbaix 2000). Masses are thus already available in the literature, namely $M_1 = 3.6 \pm 0.2 M_\odot$, $M_2 = 1.78 \pm 0.08 M_\odot$ (Ryabchikova et al. 1999) or $M_1 = 3.85 \pm 0.22 M_\odot$, $M_2 = 1.63 \pm 0.074 M_\odot$ (Pourbaix 2000).

HIP 20935 = HD 28394

This F7V star is a member of the Hyades cluster. It has a mass ratio $q = M_2/M_1$ of 0.98. However, it falls exactly along the main sequence as defined by the other stars of our sample. There is thus no indication that this star has composite colors, as it should if the companion is a main sequence F star as well. A white dwarf (WD) companion of mass $1.1 M_\odot$ is not without problems either. Böhm-Vitense (1995) has searched the IUE *International Ultraviolet Explorer* archives for spectra of F stars from the Hyades, in order to look for possible WD companions. No excess UV flux is present at 142.5 nm for HIP 20935, which implies that the WD must be cooler than

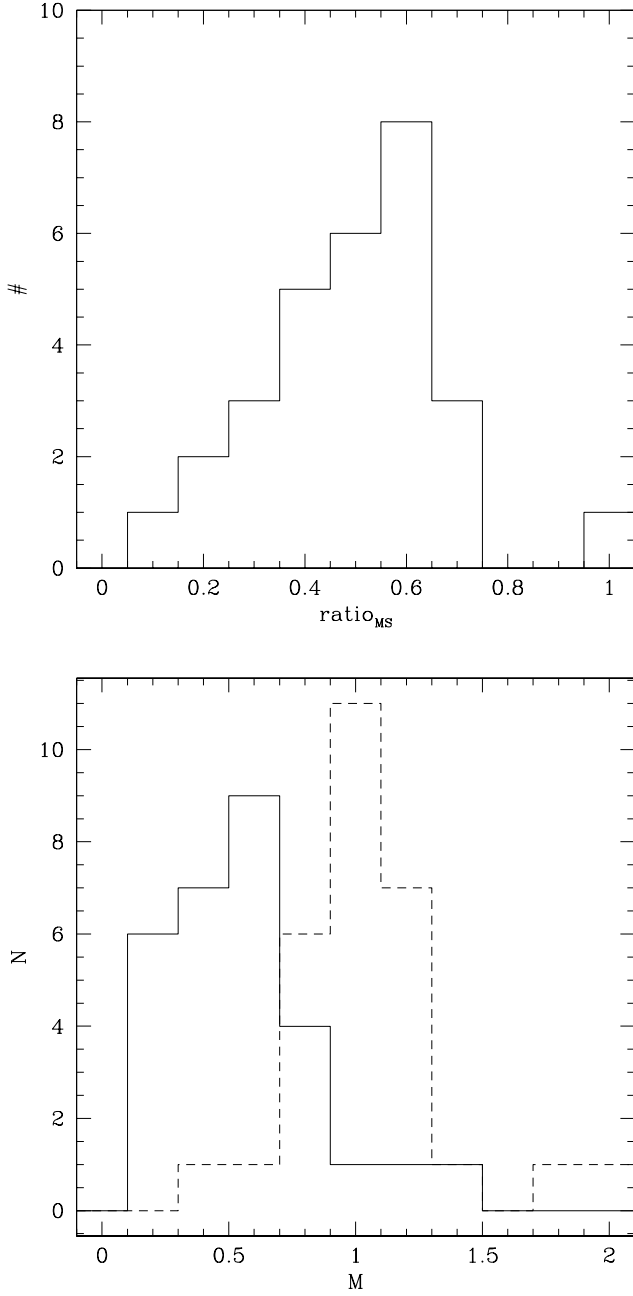


Fig. 11. Upper panel: Distribution of the mass ratio (M_2/M_1) for systems from Table 3 with a main-sequence primary star. Lower panel: Distributions of M_1 (dashed line) and M_2 (solid line).

about 10000 K. For a $1.1 M_{\odot}$ WD, this implies a cooling time of more than 1 Gyr (Chabrier et al. 2000), incompatible with the Hyades age of $800 \cdot 10^6$ y. The remaining possibility is that the companion is itself a binary with two low-luminosity red dwarfs.

HIP 105969 = HD 204613

This star is known as a subgiant CH star (Luck & Bond 1982) and the system should therefore host a WD companion (McClure 1997). Interestingly enough, the mass inferred for

this WD companion is $0.49 M_{\odot}$, just large enough for a $2 M_{\odot}$ AGB progenitor to have gone through the thermally-pulsing asymptotic granth branch phase (see Fig. 3.10 in Groenewegen 2003) to synthesize heavy elements by the s-process of nucleosynthesis. Those heavy elements were subsequently dumped onto the companion (the current CH subgiant) through mass transfer.

6.2. ($e, \log P$) diagram

With the availability of extensive sets of orbital elements for binaries of various kinds (e.g., Duquennoy & Mayor 1991 for G dwarfs, Matthieu 1992 for pre-main sequence binaries, Mermilliod 1996 for open-cluster giants, Carney et al. 2001 for blue-straggler, low-metallicity stars, Latham et al. 2002 for halo stars), it has become evident that long-period ($P > 100$ d), low-eccentricity ($e < 0.1$) systems are never found among unevolved (i.e., pre-mass-transfer) systems. This indicates that binary systems always form in eccentric orbits, and the shortest-period systems are subsequently circularized by tidal effects. On the contrary, binary systems which can be ascribed post-mass-transfer status because they exhibit signatures of chemical pollution due to mass transfer (like barium stars, some subgiant CH stars, S stars without technetium lines...) are often found in the avoidance region ($P > 100$ d, $e < 0.1$) of the ($e, \log P$) diagram. Mass transfer indeed severely modifies their orbital elements, which often end up in this region (Jorissen 2003; Jorissen & Van Eck 2005).

The companion masses derived in Sect. 6.1 offer the opportunity to check whether systems falling in the avoidance region of the ($e, \log P$) diagram could be post-mass transfer systems (most probably then with a WD companion). In total, 8 systems fall in this region, as displayed on Fig. 12: HIP 6867 (= HD 9053 = γ Phe; M0 III), HIP 8922 (= HD 11613 = HR 551; K2), HIP 10514 (= HD 13738; K3.5 III), HIP 24419 (= HD 34101; G8 V), HIP 32768 (= HD 50310 = HR 2553; K1 III), HIP 99965 (= HD 193216; G5 V), HIP 101093 (= HD 195725; A7 III) and HIP 101847 (= HD 196574; G8 III).

None of these 'avoidance-region' systems offer conclusive evidence for hosting a WD companion, but at least do not contradict it either.

HIP 6867 has a circular orbit and a rather short orbital period (193.8 d) given its late spectral type. The orbit is therefore likely to have been circularized by tidal effects rather than by mass transfer (Jorissen et al. 2004). In this specific case, there is therefore no need for the companion to be a WD.

HIP 24419 has too small a companion mass ($0.21 M_{\odot}$) to host even a He WD. This system could nevertheless have gone through a so-called 'case B' mass transfer (occurring when the primary was on the first giant branch).

For HIP 8922, HIP 10514, HIP 32768, HIP 99965, HIP 101093 and HIP 101847, we could not find in the literature any information that could help us in assessing the nature of their companion. In the case of HIP 99965 though, the companion's mass of $0.56 M_{\odot}$ would certainly not dismiss it of being a WD.

Table 6. Masses and mass ratios for the 29 systems with main-sequence primaries passing all consistency tests.

HIP	M_1 (M_\odot)	M_2 (M_\odot)	M_2/M_1	$Q = \frac{M_2^3}{(M_1+M_2)^2}$	Sp. Type	Rem.
1349	0.98	0.55	0.56	0.0711	G2	
1955	1.13	0.48	0.42	0.0420	GO	
7078	1.21	0.70	0.58	0.0953	F6	
8903	1.86	1.05	0.56	0.1358	A5	
11231	1.01	0.68	0.67	0.111	G2	
12062	0.95	0.44	0.47	0.0449	G5	
20935	1.13	1.11	0.98	0.2732	F7	not a composite spectrum despite a mass ratio close to unity
24419	0.90	0.21	0.24	0.0079	G8	
34164	1.09	0.66	0.61	0.0954	G0	
39893	0.95	0.52	0.55	0.0649	G3	
47461	-	-	-	0.0863	F2	composite spectrum
63406	0.82	0.23	0.28	0.0114	G9	
72848	0.79	0.45	0.56	0.0581	K2	
73440	1.03	0.15	0.14	0.0023	G0	
75379	1.26	0.68	0.54	0.0842	F5	
79101	3.47	1.31	0.38	0.0976	B9	
80346	0.50	0.13	0.26	0.0054	M3	
80686	1.05	0.37	0.36	0.0259	G0	
82860	1.18	0.52	0.44	0.0482	F6	
86400	0.72	0.39	0.54	0.0475	K3	
87895	0.99	0.68	0.69	0.1129	G2	
89937	1.18	0.77	0.65	0.1195	F7Vvar	
95028	1.40	0.50	0.36	0.0353	F5	
95575	0.78	0.38	0.49	0.0405	K3	
99965	0.88	0.56	0.63	0.0840	G5	
105969	1.01	0.49	0.49	0.0528	Dwarf Ba/Subgiant CH	
109176	1.25	0.80	0.64	0.1233	F5	
111170	1.08	0.70	0.65	0.1083	F7	
113718	0.76	0.18	0.24	0.0067	K4	

One should mention as well that HIP 10514 and HIP 101847 are listed in the *Perkins catalog of revised MK types for the cooler stars* (Keenan & McNeil 1989) without any mention whatsoever of spectral peculiarities. They are therefore definitely not barium stars, despite falling in the 'avoidance region' of the eccentricity – period diagram generally populated by barium stars. If we are to maintain that the 'avoidance region' can only be populated by post-mass-transfer objects – thus implying that the companion to HIP 10514 and all the stars discussed in the present section *must* be WDs – then we must accept at the same time that systems following the same binary evolution channel as that of barium stars do not necessarily end up as barium stars! Or in other words, binarity would not be a sufficient condition for the barium syndrome to develop (these systems would thus add to the non-barium binary systems listed in Jorissen & Boffin 1992).

7. Conclusions

The major result of this paper is that the detectability of an astrometric binary using the IAD is mainly a function of the orbital period (at least when the parallax exceeds 5 mas, *i.e.*, about 5 times the standard error on the parallax): detection rates are close to 100% in the period range 50 – 1000 d (corresponding to the mission duration) for systems *not* involving components with almost equal brightnesses (*i.e.*, SB2 systems or systems with composite spectra). These are more difficult to detect, because the photocenter motion is then much smaller than the actual component's motion.

A consistency test between Thiele-Innes and Campbell solutions has been designed that allowed us to (i) identify wrong spectroscopic solutions, and (ii) retain 70 systems with accurate orbital inclinations (among those, 29 involve main sequence primaries and 41 giant primaries). Among those 70 retained solutions, 20 are new astrometric binaries, not listed in the DMSA/O.

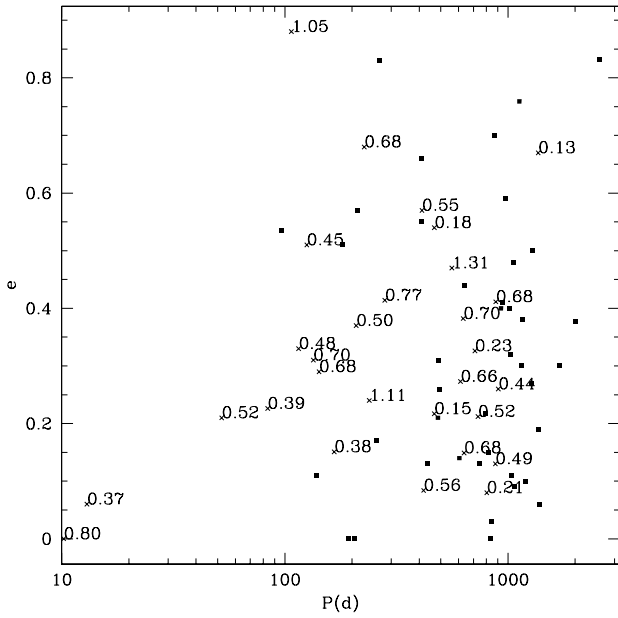


Fig. 12. The $(e, \log P)$ diagram for the 70 systems with reliable astrometric orbital elements. Systems with giant primaries are represented by black squares, and main-sequence primaries with crosses. The point labels refer to the companion mass.

This number of 70 systems passing all quality checks seems small with respect to the 122 DMSA/O systems with an S_{B9} entry. A detailed check reveals, however, that many systems present in the DMSA/O either have inaccurate astrometric orbits that would not fulfill our statistical tests, or have inaccurate spectroscopic orbital elements that make the astrometric solution unreliable anyway, or have only a_0 derived from the IAD, all other elements being taken from spectroscopic and interferometric/visual orbital elements.

Masses M_2 for the companions in the 29 systems hosting a main-sequence primary star have been derived, using the mass-luminosity relation to estimate M_1 . This was not possible for systems hosting giant primaries.

The possibility that the region $e < 0.1$, $P > 100$ d of the $(e, \log P)$ diagram is exclusively populated by post-mass transfer systems has been examined, but could not be firmly demonstrated.

Acknowledgements. AJ and DP are Research Associates, FNRS (Belgium). This research was supported in part by the ESA/PRODEX Research Grants 90078 and 15152/01/NL/SFe. We thank M. Hallin and A. Albert for discussions. We would like to thank the referee of this paper, Prof. L. Lindegren, for his very valuable comments and suggestions.

References

Abt, H. A. 1961, *ApJS*, 6, 37
 Abt, H. A. & Levy, S. G. 1976, *ApJS*, 30, 273
 Abt, H. A. & Levy, S. G. 1978, *ApJS*, 36, 241
 Aikman, G. C. L. 1976, *Publications of the Dominion Astrophysical Observatory Victoria*, 14, 379

Barker, E. S., Evans, D. S., & Laing, J. D. 1967, *Royal Greenwich Observatory Bulletin*, 130, 355
 Batten, A. H. & Fletcher, J. M. 1986, *PASP*, 98, 647
 Beavers, W. I. & Salzer, J. J. 1985, *PASP*, 97, 355
 Bertiau, F. C. 1957, *ApJ*, 125, 696
 Binnendijk, L. 1960, *Properties of Double Stars* (University of Pennsylvania Press)
 Böhm-Vitense, E. 1995, *AJ*, 110, 228
 Bopp, B. W., Evans, D. S., & Laing, J. D. 1970, *MNRAS*, 147, 355
 Bretz, M. C. 1961, *ApJ*, 133, 139
 Carney, B. W., Latham, D. W., Laird, J. B., Grant, C. E., & Morse, J. A. 2001, *AJ*, 122, 3419
 Chabrier, G., Brassard, P., Fontaine, G., & Saumon, D. 2000, *ApJ*, 543, 216
 Christie, W. H. 1936, *ApJ*, 83, 433
 Cox, A. N. 2000, *Allen's astrophysical quantities* (Edited by Arthur N. Cox.)
 Crawford, R. T. 1901, *Lick observatory bulletin*, 1, 29
 Duquennoy, A., Mayor, M., Andersen, J., Carquillat, J. M., & North, P. 1992, *A&A*, 254, L13+
 Duquennoy, A., Tokovinin, A. A., Leinert, C., et al. 1996, *A&A*, 314, 846
 Eichhorn, H. 1989, *Bull. Astron. Inst. Czechosl.*, 40, 394
 ESA. 1997, *The Hipparcos and Tycho Catalogues* (ESA SP-1200)
 Fekel, F. C. & Tomkin, J. 1983, *PASP*, 95, 1000
 Franklin, K. L. 1952, *ApJ*, 116, 383
 Ginestet, N., Carquillat, J. M., & Pedoussaut, A. 1991, *A&AS*, 91, 265
 Ginestet, N., Carquillat, J. M., Pedoussaut, A., & Nadal, R. 1985, *A&A*, 144, 403
 Griffin, R. F. 1979, *The Observatory*, 99, 36
 Griffin, R. F. 1980, *The Observatory*, 100, 161
 Griffin, R. F. 1981a, *Journal of Astrophysics and Astronomy*, 2, 115
 Griffin, R. F. 1981b, *The Observatory*, 101, 175
 Griffin, R. F. 1982a, *MNRAS*, 200, 1161
 Griffin, R. F. 1982b, *The Observatory*, 102, 27
 Griffin, R. F. 1983, *The Observatory*, 103, 17
 Griffin, R. F. 1985, *Journal of Astrophysics and Astronomy*, 6, 77
 Griffin, R. F. 1986, *The Observatory*, 106, 35
 Griffin, R. F. 1987, *The Observatory*, 107, 248
 Griffin, R. F. 1991, *The Observatory*, 111, 108
 Griffin, R. F. 1992, *The Observatory*, 112, 219
 Griffin, R. F. 2002a, *The Observatory*, 122, 14
 Griffin, R. F. 2002b, *The Observatory*, 122, 329
 Griffin, R. F., Carquillat, J.-M., & Ginestet, N. 2002, *The Observatory*, 122, 90
 Griffin, R. F. & Eitter, J. J. 1999, *The Observatory*, 119, 320
 Griffin, R. F. & Eitter, J. J. 2000, *The Observatory*, 120, 260
 Griffin, R. F., Griffin, R. E. M., Gunn, J. E., & Zimmerman, B. A. 1985, *AJ*, 90, 609
 Griffin, R. F. & Radford, G. A. 1977, *The Observatory*, 97, 196
 Grobben, J. & Michaelis, R. P. 1969, *Ric. Astr. Spec. Vatic.*, 8, 33
 Groenewegen, M. 2003, in *Asymptotic Giant Branch Stars*, ed.

- H. Habing & H. Olofsson (New York: Springer Verlag), 105
- Jackson, E. S., Shane, W. W., & Lynds, B. T. 1957, *ApJ*, 125, 712
- Jones, R. B. 1931, *Lick Observatory Bulletin*, 15, 120
- Jorissen, A. 2003, in *Asymptotic Giant Branch Stars*, ed. H. Habing & H. Olofsson (New York: Springer Verlag), 461–518
- Jorissen, A. & Boffin, H. M. J. 1992, in *Binaries as Tracers of Stellar Formation*, ed. A. Duquennoy & M. Mayor (Cambridge: Cambridge University Press), 110
- Jorissen, A., Famaey, B., Dedecker, M., et al. 2004, in *Revista Mexicana de Astronomia y Astrofisica Conference Series*, 71–72
- Jorissen, A. & Van Eck, S. 2005, in *Cosmic Abundances as Records of Stellar Evolution and Nucleosynthesis* (San Francisco: Astron. Soc. Pacific Conf. Ser.), in press
- Keenan, P. C. & McNeil, R. C. 1989, *ApJS*, 71, 245
- Kovalevsky, J. & Seidelmann, P. K. 2004, *Fundamentals of astrometry* (Cambridge: Cambridge Univ. Press)
- Latham, D. W., Mazeh, T., Stefanik, R. P., et al. 1992, *AJ*, 104, 774
- Latham, D. W., Stefanik, R. P., Torres, G., et al. 2002, *AJ*, 124, 1144
- Lehmann, H., Andrievsky, S. M., Egorova, I., et al. 2002, *A&A*, 383, 558
- Lindgren, L., Mignard, F., Söderhjelm, S., et al. 1997, *A&A*, 323, L53
- Luck, R. E. & Bond, H. E. 1982, *ApJ*, 259, 792
- Lucy, L. B. & Sweeney, M. A. 1971, *AJ*, 76, 544
- Lunt, J. 1924, *Annals of the Cape Observatory*, 10
- Lupton, R. 1993, *Statistic in theory and practice* (Princeton University Press)
- Luyten, W. J. 1936, *ApJ*, 84, 85
- Matthieu, R. D. 1992, in *Binaries as Tracers of Stellar Formation*, ed. A. Duquennoy & M. Mayor (Cambridge: Cambridge University Press), 155
- McClure, R. D. 1997, *PASP*, 109, 536
- McClure, R. D. & Woodsworth, A. W. 1990, *ApJ*, 352, 709
- Nidever, D. L., Marcy, G. W., Butler, R. P., Fischer, D. A., & Vogt, S. S. 2002, *ApJS*, 141, 503
- Pan, X., Shao, M., Colavita, M. M., et al. 1992, *ApJ*, 384, 624
- Parsons, S. B. 1983, *ApJS*, 53, 553
- Plummer, H. C. 1908, *Lick Observatory Bulletin*, 5, 24
- Pourbaix, D. 2000, *A&AS*, 145, 215
- Pourbaix, D. 2004, in *Spectroscopically and Spatially Resolving the Components of the Close Binary Star*, ASP Conference Series # 318, ed. R. Hidlitch, H. Hensberge, & K. Pavlovski, 132
- Pourbaix, D. 2005, *Gaia internal report*, DMS-DP-02
- Pourbaix, D. & Arenou, F. 2001, *A&A*, 372, 935
- Pourbaix, D. & Boffin, H. M. J. 2003, *A&A*, 398, 1163
- Pourbaix, D. & Jorissen, A. 2000, *A&AS*, 145, 161
- Pourbaix, D., Tokovinin, A. A., Batten, A. H., et al. 2004, *A&A*, 424, 727
- Radford, G. A. & Griffin, R. F. 1975, *The Observatory*, 95, 143
- Reimers, D., Griffin, R. F., & Brown, A. 1988, *A&A*, 193, 180
- Ryabchikova, T. A., Malanushenko, V. P., & Adelman, S. J. 1999, *A&A*, 351, 963
- Scarfe, C. D. 1971, *PASP*, 83, 807
- Scarfe, C. D. & Alers, S. 1975, *PASP*, 87, 285
- Scarfe, C. D., Barlow, D. J., Fekel, F. C., et al. 1994, *AJ*, 107, 1529
- Scargle, J. D. 1982, *ApJ*, 263, 835
- Spencer Jones, H. 1928a, *MNRAS*, 88, 648
- Spencer Jones, H. 1928b, *Annals of the Cape Observatory*, 10, part 8
- Stuart, A. & Ord, J. 1994, *Kendall's advanced theory of statistics* (Edward Arnold)
- Taylor, S. F., Harvin, J. A., & McAlister, H. A. 2003, *PASP*, 115, 609
- Tokovinin, A. A. 1991, *A&AS*, 91, 497
- van Leeuwen, F. & Evans, D. W. 1998, *A&AS*, 130, 157
- Wilson, R. E. 1918, *Lick Observatory Bulletin*, 9, 116
- Wolff, S. C. 1974, *PASP*, 86, 179
- Wright, K. O. 1970, *Vistas in Astronomy*, 12, 147
- Wright, K. O. & Pugh, R. E. 1954, *Publications of the Dominion Astrophysical Observatory Victoria*, 9, 407
- Young, R. K. 1920, *Publications of the Dominion Astrophysical Observatory Victoria*, 1, 263